Apoptosis (2014) 19:491–505
DOI 10.1007/s10495-013-0938-z

ORIGINAL PAPER

Claudin-7 suppresses the cytotoxicity of TRAIL-expressing mesenchymal stem cells in H460 human non-small cell lung cancer cells

Pu Xia · Wei Wang · Yang Bai

Published online: 16 November 2013
© Springer Science+Business Media New York 2013

Abstract Evidence suggests that the cytokine tumor necrosis factor-related apoptosis-inducing ligand (TRAIL) is a promising candidate for cancer therapeutics. Studies have also shown that claudin-7 (CLDN7) expression is variably dysregulated in various malignant neoplasms, with a role in lung cancer that has not been definitively decided. This work investigated the differential sensitivity of CLDN7-overexpressing human NSCLC H460 cells to TRAIL in vitro and in mouse xenografts, and explored the molecular mechanisms responsible for these effects. NCI-H460 cells were transfected or not with green fluorescent protein-tagged CLDN7. Each group was then exposed to mesenchymal stem cells (MSCs) or red fluorescent protein-tagged MSCs transduced with lentivirus expressing membrane-bound TRAIL. The effects and related mechanisms of these treatments were evaluated in vitro, and in vivo in murine xenografts. Our results indicate that TRAIL induced apoptosis in H460 cells in vitro, and in established xenograft tumors TRAIL was associated with a decrease in tumor size, tumor weight, and circulating tumor cells. CLDN7 was found to inhibit the MEK/ERK signaling pathway, leading to inhibition of death receptor 5 (TNFRSF10B). The cytotoxicity of TRAIL was confirmed in H460 cells and in vivo, and CLDN7 suppressed the cytotoxicity of TRAIL in H460 cells. Our results indicate that TRAIL may be a useful therapy to enhance apoptosis in CLDN7-negative lung cancer cells.

Keywords Lung cancer · Claudin-7 · DR5 · TRAIL · MEK/ERK signaling pathway

Introduction

The development of various cancers has been associated with the disruption of tight junctions [1], the paracellular barriers in epithelial cells that regulate the flux of ions and proteins and maintain cellular polarity [2]. Claudins are transmembrane protein components of tight junctions, whose dysfunction may be involved in the loss of tissue cohesion during the pathogenesis of cancer [3].

In humans, claudins comprise a family of 24 closely related members [4]. Several of these have been implicated in lung carcinomas, and their expressions in these tissues have been investigated at both the protein and mRNA levels. Paschoud et al. [5] found that lung squamous cell carcinomas tested positive for claudin-1 but negative for claudin-5, while the reverse was true of adenocarcinomas. In the study of Moldvay et al. [6], significant differences in immunohistochemical claudin-2 expression were found between small cell lung carcinoma and squamous cell carcinoma.

Claudin-7 (CLDN7) is expressed in epithelial cells of several organs, largely outside the tight junction area and

Pu Xia and Wei Wang contributed equally to this work.

P. Xia (✉)
Department of Biochemistry and Molecular Biology, School of Basic Medical Science, China Medical University, Shenyang 110001, People's Republic of China
e-mail: nn001007@163.com

W. Wang
Department of Pathophysiology, School of Basic Medical Science, China Medical University, Shenyang, People's Republic of China

Y. Bai
Department of Clinical Pharmacology, College of Pharmacy, China Medical University, Shenyang, People's Republic of China

along the basolateral membrane [7, 8]. More and more studies show that abnormal CLDN7 expression is related to various malignant neoplasms, including breast carcinomas [9], colorectal cancer [10], and esophageal cancer [11]. Lu et al. [12] showed that CLDN7 expression was either downregulated or its localization was disrupted in human lung cancer tissues. In non-small cell lung cancer (NSCLC), Yamamoto et al. [13] found that reduced CLDN7 expression was associated with poor outcome, particularly in squamous cell carcinoma.

Tumor necrosis factor-related apoptosis-inducing ligand (TRAIL) is a type 2 transmembrane death ligand that causes apoptosis in various tumors and cancer cells [14–17], including human H460 non-small cell lung cancer (NSCLC) cells [18]. TRAIL binds to the death domain-containing receptors TNFRSF10A (tumor necrosis factor receptor [TNFR] superfamily, member 10a, also known as DR4) and TNFRSF10B (TNFR superfamily, member 10b, also known as DR5) and activate caspase 8, leading directly to the activation of caspase 3 and subsequent apoptosis [19, 20].

This work investigated the differential sensitivity of CLDN7-overexpressing human NSCLC H460 cells to TRAIL in vitro and in mouse xenografts, and explored the molecular mechanisms responsible for these effects. To our knowledge, no studies have previously shown the tumor-suppressive effects of MSC-delivered TRAIL or the underlying mechanisms of these effects in human NSCLC H460 cells overexpressing CLDN7.

We found that CLDN7 lowered the sensitivity to TRAIL of H460 cells by downregulating the TRAIL receptor TNFRSF10B. Intriguingly, a set of H460-secreted factors, consisting of interleukin (IL)6, IL8, matrix metalloproteinase (MMP)2, and MMP9, also changed after TRAIL treatment. In vivo mouse models confirmed that CLDN7 expression moderated the cytotoxicity of TRAIL-transduced MSCs in H460 xenograft tumors. Collectively, our results indicate that TRAIL could be used in human lung cancer therapy. However, tumors with CLDN7 expression may not be sensitive to TRAIL-induced cell death.

Materials and methods

Overview of study design

The study design comprised three broad sets of experiments. First, we examined the role of TRAIL in human lung cancer H460 cells and CLDN7-transfected H460 cells, by exposure to TRAIL-transduced mesenchymal stem cells (MSCs) and standard assays of apoptosis and subcellular localization. Second, we established H460 and CLDN7-positive H460 xenografts in mice and observed differences in tumor weight, tumor size, survival time, and circulating tumor cells (CTCs) after TRAIL treatment. ELISA was used to detect the plasma levels of TRAIL. Then the correlation between TRAIL and CTCs was confirmed. Finally, RT-PCR, immunoprecipitation and Western blot were used to determine the possible mechanisms of TRAIL in CLDN7-transfected H460 cells.

H460 cell culture and transfection

Cells of the human non-small cell lung cancer cell line NCI-H460 was purchased from the American Type Culture Collection (Manassas, VA, USA) and grown in RPMI 1640 culture medium containing 10 % fetal bovine serum, 100 units/mL of penicillin, and 100 μg/mL streptomycin in humidified air (5 % CO_2 atmosphere) at 37 °C.

A portion of the parental H460 cells were transfected with green fluorescent protein (GFP)-tagged CLDN7 (H460-GFP-CLDN7) was transfected into H460 cells using Lipofectamine 2000 Reagent (Invitrogen, Carlsbad, CA, USA). After a 48-h incubation, transfected cells were transferred from 6-well plates to 100-mm plates. To confirm and localize the presence or non-presence of CLDN7 in parental H460 cells and H460-GFP-CLDN7 cells, the subcellular localization of GFP-CLDN7 was examined under a fluorescent microscope, and RT-PCR and Western blot was performed (described below).

Mesenchymal stem cells (MSCs) transduced with TRAIL

Mesenchymal stem cells (MSCs) have been used as delivery vehicles for targeted anti-tumor therapies [21, 22]. MSCs (a kind gift from Dr. Jin-Jin Wang) were transduced or not with membrane-bound TRAIL and red fluorescent protein (RFP) using a lentivirus (RFP-MSC-TRAIL), as previously described by Loebinger et al. [22]. RT-PCR, Western blot, and ELISA were performed (described below) to confirm the differential presence of TRAIL in the MSC and RFP-MSC-TRAIL treatment groups.

Coculture

A dividing partition was inserted into a well of 6-well dishes (Fig. 4a). Parental (i.e., non-transduced) MSCs or RFP-MSC-TRAIL cells were plated into one compartment of the well (3×10^5 cells/well) in the culture media described above. H460 or H460 CLDN7-GFP cells were plated into the other compartment of the well (3×10^5 cells/well). After 24 h, the bulkhead was removed. Differential migrations of RFP-MSC-TRAIL cells toward the H460 and H460-GFP-H460 cells were

noted. The 4 treatment groups of cells after coculture were used in the following studies.

Cytotoxicity/cellular proliferation MTT assay

To determine the cytotoxic effect of exposure to TRAIL on H460 and CLDN7-GFP-H460 cells compared with untreated (control) H460 cells, cellular proliferation was assessed using a 3-(4,5-dimethylthiazol-2-yl)-2,5-diphenyltetrazolium bromide (MTT) assay. Cells (2×10^3 per well) after coculture were plated into 96-well microtiter plates and allowed to adhere. MTT (10 μL, at 5 mg/mL) was added to each well at a final concentration of 500 μg/mL. The mixture was further incubated for 1 h at 37 °C, and the liquid in the wells was removed. Four hours later, cells were lysed with dimethyl sulfoxide (DMSO) and absorbance rates were measured at 550-560 nm using a microplate reader (Bio-Rad, Hercules, CA, USA).

Quantitative analysis of apoptosis with annexin V-fluorescein isothiocyanate (FITC)/propidium iodide (PI) double staining and flow cytometry

To further determine the cytotoxic effect of exposure to TRAIL on H460 and CLDN7-GFP H460 cells compared with untreated (control) H460 cells, differential apoptotic rates were determined with annexin V-FITC/PI double staining assays. In accordance with the manufacturer's instructions (Apoptosis Detection Kit, KeyGEN, Nanjing, China), cells were washed and resuspended in binding buffer prior to the addition of FITC-labeled annexin V and PI for 10 min. Suspensions were immediately analyzed by flow cytometry using a FACSCalibur machine (BD Biosciences, Baltimore, MD, USA). Cells in the stages of early apoptosis were defined as $FITC^+/PI^-$ cells. Survival rates of H460 cells in monoculture (%) were subtracted from the percentage of surviving H460 cells in the coculture, to determine the relative survival advantage.

Caspase assay

The cytotoxic effect of exposure to TRAIL on H460 and CLDN7-GFP H460 cells compared with untreated (control) H460 cells was also investigated by measuring caspase 3 and caspase 9 activity (indicators of apoptosis) using caspase colorimetric assay kits in accordance with the manufacturer's instructions (KeyGEN). Briefly, cellular protein was extracted using the lysis buffer supplied, and total protein concentrations were determined with a Bradford protein assay. Caspase 3 or caspase 9 substrate was then added, and after 2 h at 37 °C in the dark, caspase 3 or caspase 9 was measured using a microtiter plate reader at 405 nm.

Cytokine array

H460 or H460 CLDN7-GFP cells were left untreated, or (described below) were treated with recombinant human TRAIL (100 ng/mL, R&D Systems) for 48 h. As per the manufacturer's recommended protocol, a cytokine/chemokine array kit (Ray Biotech, Norcross, GA, USA) was used to detect a panel of 13 secreted cytokines and chemokines: IL1A, IL1B, IL2-8, IL17, MMP2, MMP9, and TRAIL.

Detection of cell surface TNFRSF10A and TNFRSF10B via flow cytometry

The procedure determining the H460 or H460 CLDN7-GFP cell surface expression of the TRAIL receptors TNFRSF10A and TNFRSF10B was in accordance with the manufacturer's recommendations (R&D Systems, Minneapolis, MN, USA). In brief, cells were harvested by trypsinization and washed twice in ice-cold phosphate-buffered saline (PBS). After washing, cells were incubated with anti-TNFRSF10A or anti-TNFRSF10B mouse antibody (dilution ratio 1:50) overnight at 4 °C. Afterwards, cells were washed again three times with PBS, and incubated with FITC/phycoerythrin (PE)-conjugated goat anti mouse IgG (dilution ratio 1:50) for 40 min in the dark at room temperature. Finally, cells were washed three times with PBS and resuspended in 0.5 mL PBS for flow cytometry.

Immunoprecipitation

To determine whether CLDN7 and TRAIL interact with each other, we performed immunoprecipitation. Transfected cells were washed once with PBS, lysed for 30 min in lysis buffer (50 mM Tris–HCl pH 7.5, 150 mM NaCl, 1 % Nonidet P-40) containing protease inhibitors (Cocktail, Roche, Basel, Switzerland) and phosphatase inhibitors (1 mM NaF and 1 mM $Na3VO_4$), and centrifuged at 15 000 × *g* at 4 °C for 15 min. Supernatants were pre-cleared with EZ View Red protein G-Sepharose (Sigma) for 1 h at 4 °C, and 5 μg of antibody specific for each target protein were added in each sample. Immune complexes were precipitated by EZ View red protein G-Sepharose overnight at 4 °C and washed 3 times with lysis buffer. The immune complexes were boiled (100 °C) for 10 min in SDS sample buffer (100 mM Tris–HCl pH 8.8, 0.01 % bromophenol blue, 20 % glycerol, 4 % SDS) containing 10 mM dithiothreitol, and resolved via 10 % SDS-PAGE.

In vivo effects of TRAIL on H460-GFP-CLDN7 xenografts

Our University Ethics Committee approved the research protocols performed in this study. NOD SCID mice (4 to

6-weeks-old, NOD.CB17-Prkdcscid/NcrCrl; Charles River, Wilmington, MA, USA, 30 mice in each treatment group) were injected subcutaneously with H460 (1×10^7 cells in 200 μL PBS), or H460-GFP-CLDN7 cells (1×10^7 cells in 200 μL PBS) mixed with MSCs (1×10^7 cells) or TRAIL-transfected MSCs (RFP-MSC-TRAIL; 1×10^7 cells) into the axilla of each mouse. The mice were examined at 0, 10, 20, 30, 40, 50, and 60 days, and tumor growth was evaluated by measuring the length and width of the tumor mass after euthanasia. The tumors were resected and the tumor weight and volume were determined. Tumors were measured using calipers, and tumor volumes were calculated (tumor volume = length $\times$ width^2 $\times$ 0.52) [23].

Survival curves

One hundred mice were used to establish xenografts for observing survival time (20 mice in each treatment group: H460; H460-GFP-CLDN7 cells; H460 mixed with MSCs; H460 mixed with TRAIL-transfected MSCs; H460-GFP-CLDN7 cells mixed with TRAIL-transfected MSCs. The survival status of the mice was observed until the experiments were terminated, at which time all the mice had died except for those in the H460 mixed with TRAIL-transfected MSCs group.

Isolation and enumeration of CTCs

The CellSearch system (Veridex, Warren, NJ, USA) is the only test sanctioned by the United States Food and Drug Administration for enumeration of CTCs in clinical practice [24]. Blood samples (1 mL) from mouse models were drawn into CellSave tubes, which were maintained at room temperature and processed within 72 h of collection. CTCs were defined as nucleated epithelial cell adhesion molecule (EpCAM)-positive cells, lacking cluster of differentiation (CD) 45 but expressing cytoplasmic cytokeratins 8, 18, and 19. All CTC evaluations were performed by qualified and trained personnel. To further investigate the association between the number of CTCs and prognosis, we defined 3 risk groups; low (CTC $<$ 1), medium (CTC 1–5), and high risk (CTC $>$ 5).

Enzyme-linked immuno sorbent assay (ELISA)

Blood samples for TRAIL determination were collected in ethylenediaminetetraacetate tubes, placed on ice, and centrifuged at 2,500$\times g$ for 20 min. Recovered serum was stored at −80 °C in aliquots until assayed. For the measurement of circulating TRAIL, analyses were performed in duplicate using a dedicated, commercially available ELISA kit (R&D Systems) in accordance with the manufacturer's instructions, and analyzed with an ELISA reader at 450 nm.

RNA isolation and reverse transcriptase-polymerase chain reaction (RT-PCR)

RT-PCR was performed during the in vitro studies to confirm the non-presence of *CLDN7* mRNA in parental H460 cells and H460-GFP-CLDN7 cells, to confirm the differential presence of *TRAIL* mRNA in MSCs and the RFP-MSC-TRAIL cells, and to determine expression levels of the functional TRAIL receptors (TNFRSF10A and TNFRSF10B) (in vivo experiments).

Total RNA was isolated from cells using an RNeasy Mini Kit (Biomed, Beijing, China). RNA (1 μg) was reverse-transcribed using avian myeloblastosis virus (AMV) reverse transcriptase (Promega, Madison, WI, USA) and amplified using specific primers and conditions for target genes. The *TRAIL* primers were: 5′-CCCAAT GACGAAGAGAGTATGA-3′ (sense) and 5′-GGAATAG ATGTAGTAAAACCC-3′ (antisense). The *CLDN7* primers were: 5′-GGGTGGAGGCATAATTTTCA-3′ (sense) and 5′-AGTGCACCTCCCAGGATGAC-3′ (antisense). The *TNFRSF10A* primers were: 5′-CAGAGGGATGGTCAAGG TCAAGG-3′ (sense) and 5′-CCACAACCTGAGCCGATG C-3′ (antisense). The *TNFRSF10B* primers were: 5′-CACCA GGTGTGATTCAGGTG-3′ (sense) and 5′-CCCCACTGTG CTTTGTACCT-3′ (antisense). Glyceraldehyde-3-phosphate dehydrogenase (*GAPDH*) was used as an internal normalization control. The *GAPDH* primers were: 5′-GAAGGCTG GGGCTCATTT-3′ (sense) and 5′-GGGGCCATCCAC AGTCTT-3′ (antisense).

PCR amplification of cDNA was performed in reaction volumes of 15 μL. Finally, products were resolved by 1 % agarose gel electrophoresis, and visualized by ethidium bromide staining and an ultraviolet imaging system (UVP, Upland, CA, USA).

Western blot

Western blot was performed to determine which pathways are affected by TRAIL in H460 or H460-GFP-CLDN7 cells. Cells were lysed as described above (under *Immunoprecipitation*). Tumor tissues were obtained from mouse models and lysed as described in Immunoprecipitation. Crude lysates were then centrifuged at 14,000$\times g$ for 10 min, and cleared lysates were collected and separated by 10 % SDS-polyacrylamide gel electrophoresis and transferred to nitrocellulose membranes. Membranes were blocked in 5 % milk-Tris-buffered saline with Tween-20 and incubated with primary antibodies. Anti-TRAIL and anti-CLDN7 antibodies (Santa Cruz Biotechnology, Santa Cruz, CA, USA) were used to identify transfection

efficiency, and detection of β-actin was used as an internal control.

Cell signaling-related proteins obtained from tumor tissues were probed using the following antibodies: anti-TNFRSF10A, anti-TNFRSF10B, anti-caspase 8, anti-caspase 9, anti-caspase 3, fas-associated protein with death domain (FADD), anti-ERK, anti-phospho-extracellular-signal-regulated kinase (ERK), anti-MEK, and anti-phospho-MEK antibodies (Santa Cruz). The reaction was followed by probing with peroxidase-coupled secondary antibodies including anti-mouse IgG, anti-rabbit IgG, or anti-goat IgG antibodies at dilutions ranging from 1:1,000 to 1:2,000 (Amersham Biosciences, Needham, MA, USA), and binding results were visualized via enhanced chemiluminescence (Amersham Pharmacia, Piscataway, NJ, USA).

TNFRSF10B small interfering RNA (siRNA) and MAP2K (MEK) siRNA

To further verify the role of the MEK/ERK signaling pathway, *TNFRSF10B* and *MAP2K* (*MEK*) siRNA were applied to H460 or H460-GFP-CLDN7 cells and reproduced the experiments described above. TNFRSF10B siRNA was purchased from Qiagen (Doncaster, Victoria, Australia), with a mixture of two target sequences (ACC AGGTGTGATTCAGGTGAA and CCGACTTCACTTG ATACTATA for TNFRSF10B). *MAP2K (MEK)* siRNA was purchased from Cell Signaling Technology (Beverly, MA, USA). The siRNA were transfected using HiPerfect transfection reagent (Qiagen) in accordance with the manufacturer's protocol.

Statistical analyses

Data were recorded from three independent experiments. Statistical analyses were performed with GraphPad Prism 5 (GraphPad Software, La Jolla, CA, USA). $P < 0.05$ was considered statistically significant, and error bars throughout indicate standard error of the mean. A paired *t* test was used for normalized data, and nonparametric data were analyzed using the Wilcoxon matched-pairs test followed by Mann–Whitney test. Correlation was determined using Spearman's nonparametric correlation. The Kaplan–Meier estimator was used to compare different patient groups, and *P*-values were calculated using the log-rank (Mantel-Cox) test.

Results

Transfection of CLDN7 in H460 cells and TRAIL in MSC cells

We transfected NCI-H460 cells with GFP-tagged CLDN7 (H460-GFP-CLDN7) or did not (H460). The subcellular localization of overexpressed GFP-CLDN7 was examined under a fluorescent microscope. The GFP-CLDN7 signal was observed at the membrane (Fig. 4a).

In parental (non-transfected) H460 cells there was no detectable endogenous *CLDN7* mRNA as determined by RT-PCR, or protein CLDN7 determined Western blot when compared to H460-GFP-CLDN7 cells (Fig. 1a, b).

RFP-labeled MSCs transfected with TRAIL (RFP-MSC-TRAIL) proliferated, as shown by the MTT assay. Levels of TRAIL were detected using RT-PCR and Western blot

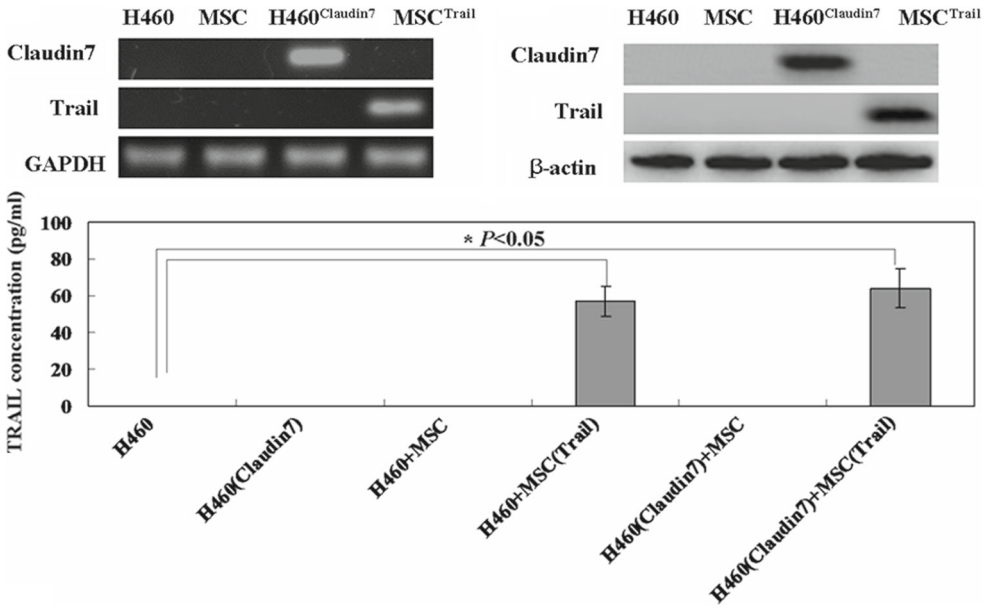

Fig. 1 The transfection of CLDN7 in H460 cells and TRAIL in MSC cells, respectively. **a** The mRNA levels of *CLDN7* and *TRAIL* were determined by RT-PCR. *GAPDH* was used as an internal control. **b** The expression of CLDN7 and TRAIL protein was determined by Western blot. β-actin expression was used as an internal control. **c** Results of ELISA show the level of TRAIL produced in TRAIL-expressing MSCs

assays. In both RT-PCR and Western blot assays, levels of TRAIL mRNA and TRAIL protein were lower in non-transfected MSCs compared with transfected MSCs (Fig. 1a, b). Secreted TRAIL protein was significantly higher in transfected cells than non-transfected ones using ELISA (Fig. 1c; $P < 0.05$).

Effects of TRAIL-transfected MSCs on the proliferation, apoptosis, cytokine secretion, and mobility of H460 or CLDN7-GFP H460 cells

After the coculture experiments (Fig. 4a), we found that the proliferation rate of H460 cells was significantly decreased after treatment with TRAIL (Fig. 2a; $P < 0.05$). However, the proliferation rate of CLDN7-GFP H460 cells did not statistically differ from that of H460 cells (Fig. 2a). TRAIL showed no significant effects on CLDN7-GFP H460 cells (Fig. 2a).

Quantitative analysis of apoptosis was conducted via annexin V/PI double staining and flow cytometry. The treatment of H460 cells with TRAIL resulted in a significant difference in the apoptotic ratio when compared with non-treated H460 cells ($P < 0.05$; Fig. 2b). H460-GFP-CLDN7 cells treated with TRAIL showed no higher apoptotic ratio than did the non-treated H460-GFP-CLDN7 cells.

We also analyzed the activities of caspase 3 and 9 in H460 and CLDN7-GFP H460 cells, and found that TRAIL treatment resulted in significantly higher caspase 3 and 9 activities compared with untreated H460 cells ($P < 0.05$; Fig. 2d). However, CLDN7 inhibited TRAIL-induced activation of caspase 3 and 9 in H460 cells (Fig. 2c).

H460 cells secreted the cytokines IL6, IL8, MMP2 and MMP9 (Fig. 2d). H460claudin7 cells did not secrete MMP2 and MMP9 but secreted lower levels of IL6 and IL8 than did H460 cells. In contrast, a slightly increased

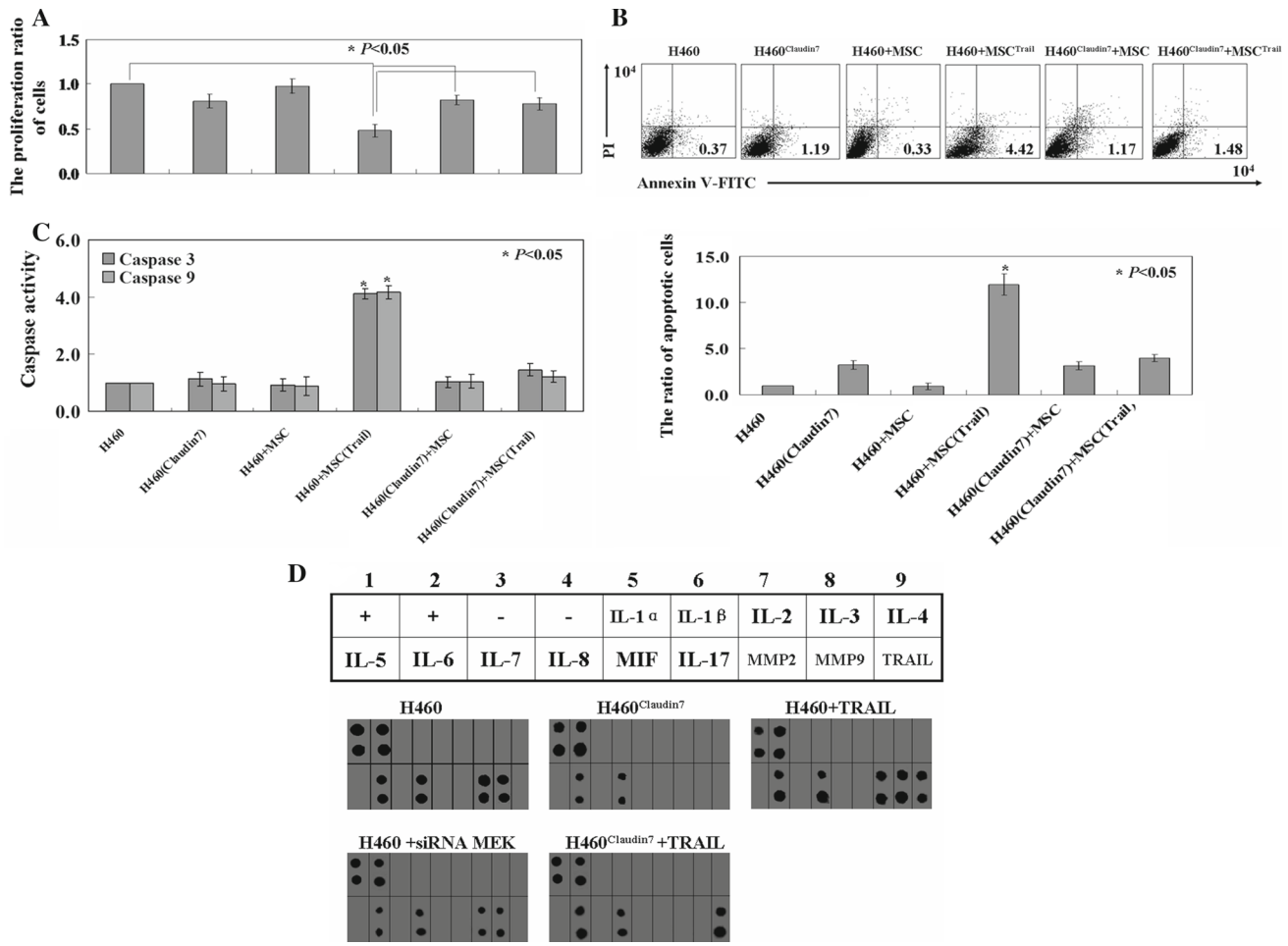

Fig. 2 CLDN7 moderates the cytotoxicity of TRAIL to H460 cells in vitro. **a** The *growth curve* of cell lines was determined by MTT assay. **b** The proportion of apoptotic cells (early apoptosis) was determined by double-staining with annexin V/FITC and PI. **c** The activity of caspase 3 and 9 was detected in each group as described in "Materials and methods" section. **d** A typical secretion profile of H460 cells using the cytokine array membrane. The positive and negative controls are placed at *upper left* corner

secretion of IL6, IL8, MMP2, and MMP9 were detected in H460 cells after TRAIL treatment. However, when H460 cells were treated with MEK siRNA, a decreased secretion of the four cytokines was detected (Fig. 2d).

Changes in TNFRSF10B and TNFRSF10A levels after TRAIL treatment in H460 or CLDN7-GFP H460 cells

The expression levels of the functional TRAIL receptors were examined using RT-PCR (Fig. 3a), Western blot (Fig. 3b), and flow cytometry (Fig. 3c). We confirmed that both *TNFRSF10B* and *TNFRSF10A* mRNA and TNFRSF10B and TNFRSF10A protein levels in H460 cells with TRAIL treatment showed no changes compared with that of non-treated H460 cells (Fig. 3a, b). However, a redistribution of TNFRSF10B on the plasma membrane of H460 cells with TRAIL treatment was observed by flow cytometry (Fig. 3c). Interestingly, H460-GFP-CLDN7 showed lower levels of TNFRSF10A and TNFRSF10B than did H460 cells (Fig. 3).

TRAIL-transfected MSCs migrate toward CLDN7-GFP H460 cells

The ability of TRAIL-transfected MSCs to migrate toward lung cancer cells was detected using a dividing partition that was inserted into a well of 6-well dishes (Fig. 4a). H460-GFP-CLDN7 cells and H460 cells were used to attract TRAIL-transfected MSCs, and non-transfected MSCs used as a control. There was a significantly increased migration of TRAIL-transfected MSCs toward the CLDN7-GFP H460 cells, but no significantly increased migration toward the H460 (Fig. 4a).

To investigate why H460-GFP-CLDN7 cells could attract TRAIL-transfected MSCs, we performed immunofluorescence and co-immunoprecipitation studies. First, we utilized immunofluorescence to determine the cellular localization of CLDN7 and TRAIL between CLDN7-GFP H460 cells and TRAIL-transfected MSCs. It seems that CLDN7 and TRAIL co-localized in the cell membrane (Fig. 4b).

To determine whether CLDN7 and TRAIL could interact with each other, we performed co-immunoprecipitation and Western blot analyses. No interaction between CLDN7 and TRAIL was found using co-immunoprecipitation analysis (Fig. 4c).

TRAIL-expressing MSCs reduce subcutaneous tumor growth in mice

In contrast to the above in vitro cell proliferation data, we next determined whether TRAIL displays anti-tumor properties in established xenograft tumor models. As in the in vitro experiments, CLDN7 reduced the cytotoxicity of TRAIL in H460 cells (Fig. 5).

TRAIL-expressing MSCs resulted in a significantly reduced tumor size and weight in nude mice carrying H460 carcinoma. However, there was no change in the tumor growth in nude mice carrying CLDN7-GFP H460 cells carcinoma ($P < 0.05$; Fig. 5b, c). We also found that the TRAIL-treated H460 group had a better survival rate compared to that of the non-treated H460, non-treated CLDN7-GFP H460 cells, and TRAIL-treated CLDN7-GFP H460 groups ($P < 0.05$; Fig. 5d). We isolated and enumerated the circulating tumor cells in mouse models by using the CellSearch system. Those in the TRAIL-treated H460 group showed fewer CTCs in their peripheral blood

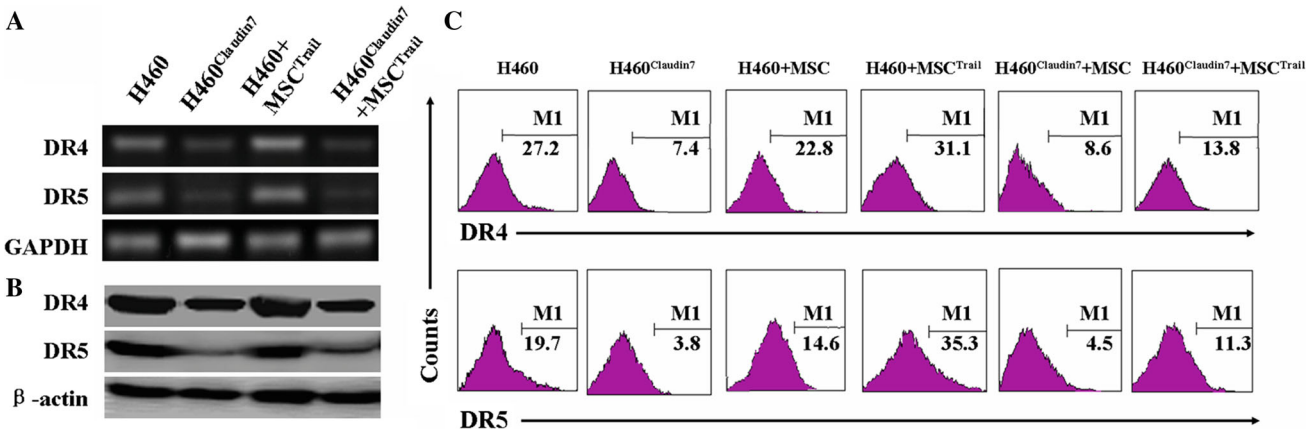

Fig. 3 The death receptor expression levels of H460 cells. **a** The mRNA levels of *TNFRSF10A* and *TNFRSF10B* in H460 cells were detected by RT-PCR. **b** The protein levels of TNFRSF10A and TNFRSF10B in H460 cells were detected by Western blot. **c** The cell surface expressions of TNFRSF10A and TNFRSF10B in H460 cells were detected by flow cytometry

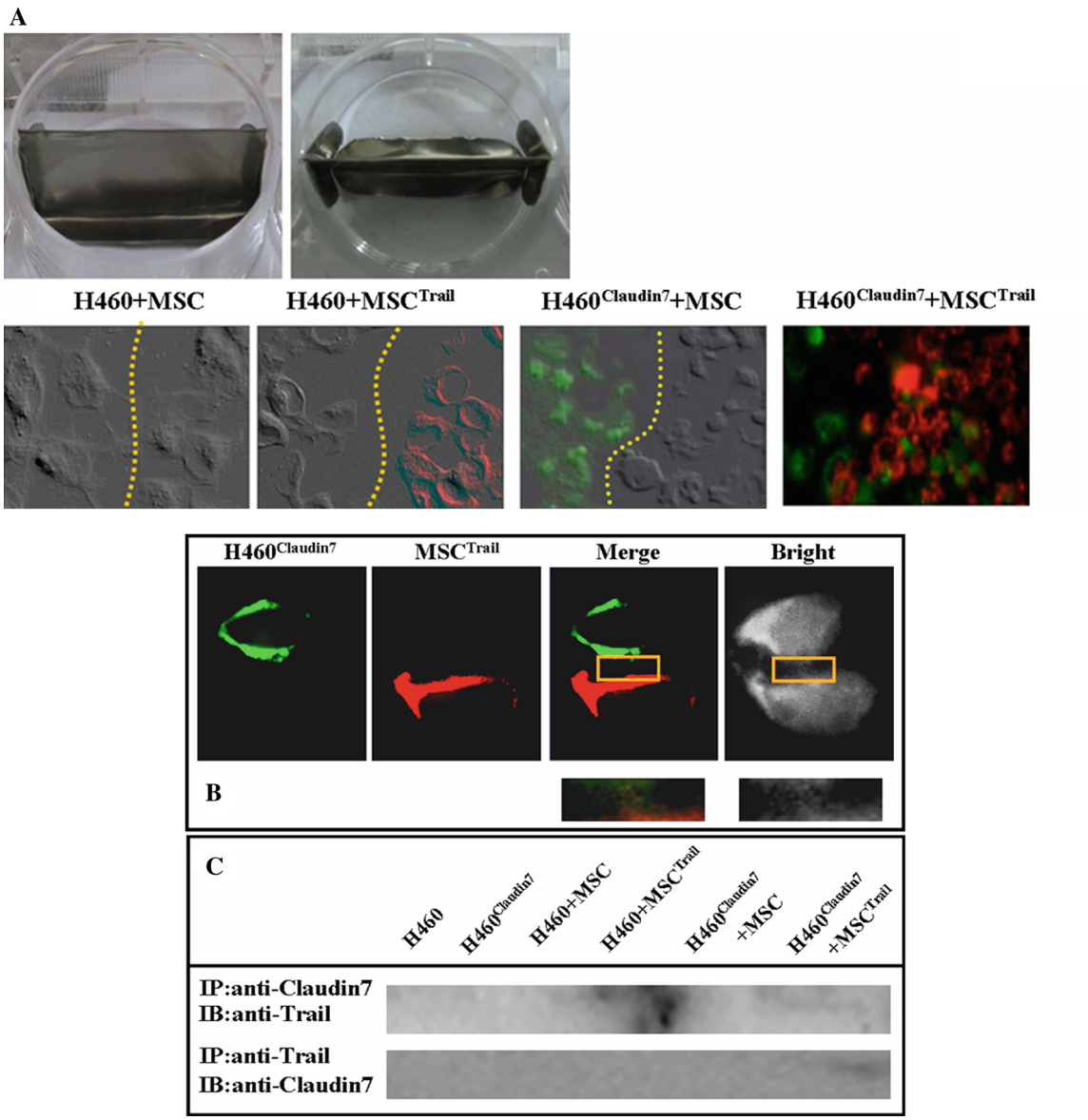

Fig. 4 TRAIL did not interact with CLDN7. **a** The migration results show that H460-GFP-CLDN7 and MSC-RFP-TRAIL cells significantly promote reduction in gap size caused by cell migration. **b** Immunofluorescence showed localization of TRAIL and CLDN7. *Red* TRAIL-transduced MSCs, *green* CLDN7-GFP expressing H460 cells. **c** Protein extracts from MSC-RFP-TRAIL cells or H460-GFP-CLDN7 cells were immunoprecipitated with anti-TRAIL or anti-CLDN7 antibodies and immunoblotted with anti-CLDN7 or anti-TRAIL antibodies as indicated (Color figure online)

than did those in the other groups ($P < 0.05$; Fig. 6a). Slightly fewer CTCs were in the CLDN7-GFP H460 and TRAIL-treated CLDN7-GFP H460 groups than in the H460 group ($P < 0.05$; Fig. 6a).

To further investigate the association between the number of CTCs and prognosis, we defined 3 risk groups; low (CTC < 1), medium (CTC 1–5), and high risk (CTC > 5). A significantly different survival rate between the low and the medium risk as well as between the medium and the high risk groups in the Cox model was confirmed ($P < 0.05$; Fig. 6b). The TRAIL-expressing MSC-treated group had a higher serum TRAIL level than did the non-treated group ($P < 0.05$; Fig. 6c). When the TRAIL-treated CLDN7-GFP H460 group was excluded, the plasma levels of TRAIL and the number of CTCs were significantly negatively correlated in the other four groups ($r = -0.554$, $P < 0.05$; Fig. 6d). However, when all groups were included, no association was observed between TRAIL levels and CTCs ($r = -0.153$, $P > 0.05$; Fig. 6e). This result further confirmed that CLDN7 could inhibit the effects of TRAIL on H460 cells.

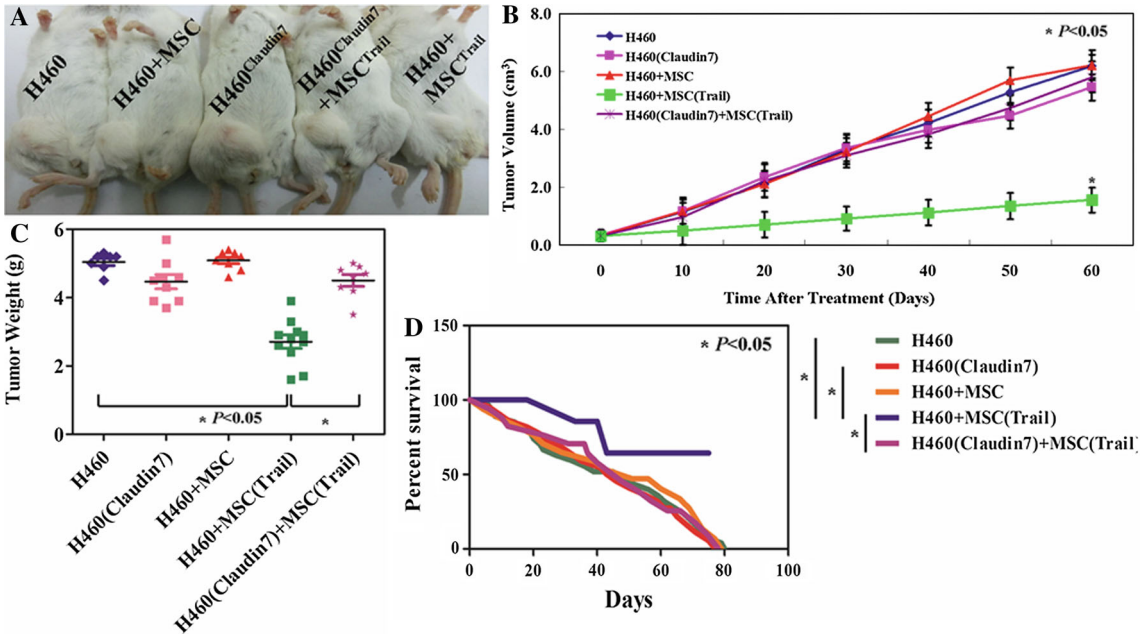

Fig. 5 The role of CLDN7 and TRAIL in xenograft mouse models. **a** Macroscopic appearance of subcutaneous tumors in each group described in "Materials and methods" section. **b**, **c** Tumor volume and tumor weights of each group described in "Materials and methods" section. **d** Kaplan–Meier survival curves of the groups described in "Materials and methods" section

MEK or TNFRSF10B knockdown affects TRAIL-induced apoptosis in H460 cells

As described above, we found that CLDN7 could inhibit TRAIL-induced apoptosis in H460 cells, and that CLDN7 could downregulate TNFRSF10B expression in H460 cells. We hypothesized that the distinct sensitivity of H460 and CLDN7-GFP cells to TRAIL was due to differences in CLDN7 expression. We therefore tested the effects of TRAIL on H460 cells after TNFRSF10B knockdown through transfection with TNFRSF10B-siRNA. TRAIL showed no effects on H460 cells after TNFRSF10B knockdown both in vivo and in vitro. The proliferation rate of H460 cells with TNFRSF10B knockdown after TRAIL treatment was higher than that of H460 cells with TRAIL treatment (Fig. 7b). Whereas, H460 cells with TNFRSF10B knockdown after TRAIL treatment had a lower apoptotic rate than that of H460 cells with TRAIL treatment (Fig. 7a). Moreover, there was a lower level of caspase activity in H460 cells with TNFRSF10B knockdown after TRAIL treatment than in H460 cells with TRAIL treatment (Fig. 7d). TRAIL had no effect on tumor weight and tumor size in nude mice carrying H460 carcinoma after siRNA TNFRSF10B treatment compared with untreated mice (Fig. 8). The anti-tumor effect of siRNA targeting MEK was similar to that of siRNA targeting TNFRSF10B on H460 cells (Figs. 7, 8). Interestingly, H460 cells after treatment with siRNA MEK showed a lower TNFRSF10B expression than the non-treated H460 cells (Fig. 7).

CLDN7 suppresses TRAIL-induced apoptosis in H460 by blocking the MEK/ERK signaling pathway

To determine the mechanisms underlying inactivation of TRAIL-induced apoptosis by CLDN7, an experiment was carried out to measure changes in the MEK/ERK signaling pathway. While total levels of MEK and ERK showed no changes, the levels of phospho-MEK and phospho-ERK were observed to be higher in H460 cells compared with H460claudin7 cells (Fig. 9). To test the hypothesis that CLDN7 could block TNFRSF10B expression in H460 cells by suppressing the MEK/ERK signaling pathway, siRNA targeting TNFRSF10B or siRNA targeting MEK was used to treat H460 cells as blockers. Inhibition of phospho-MEK, phospho-ERK, MEK, and TNFRSF10B were detected in H460 cells after siRNA MEK treatment (Fig. 9, lane 3). Expression levels of other factors such as FADD, caspase 8, caspase 9, and caspase 3 were also lower and associated with the MEK knockdown (Fig. 9, lane 3). Altogether, these results suggest that CLDN7 could inhibit TRAIL-induced apoptosis in H460 cells via suppressing MEK/ERK signaling pathway.

Discussion

As noted in the Introduction, CLDN7 is a tight junction protein that has an important role in tumorigenesis, tumor invasion and metastasis [7, 8]. Yamamoto et al. [13] found that 66.7 % of non-small cell lung cancer tissues

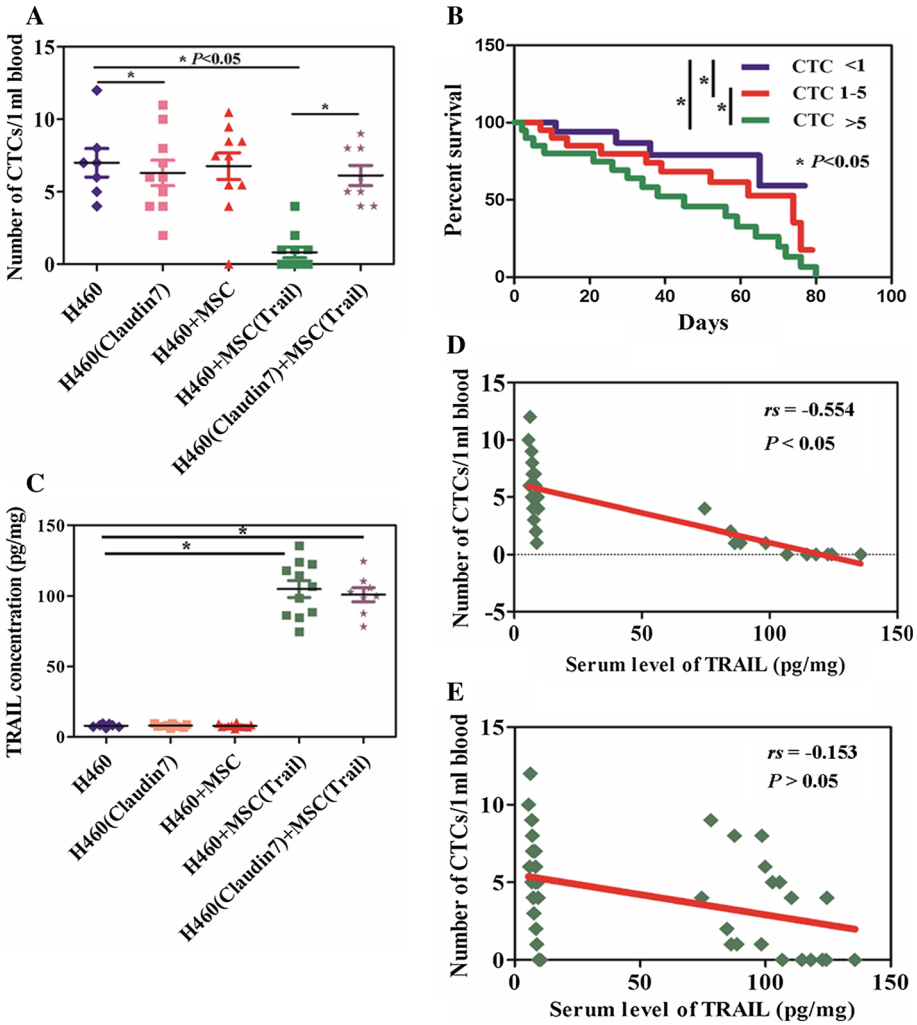

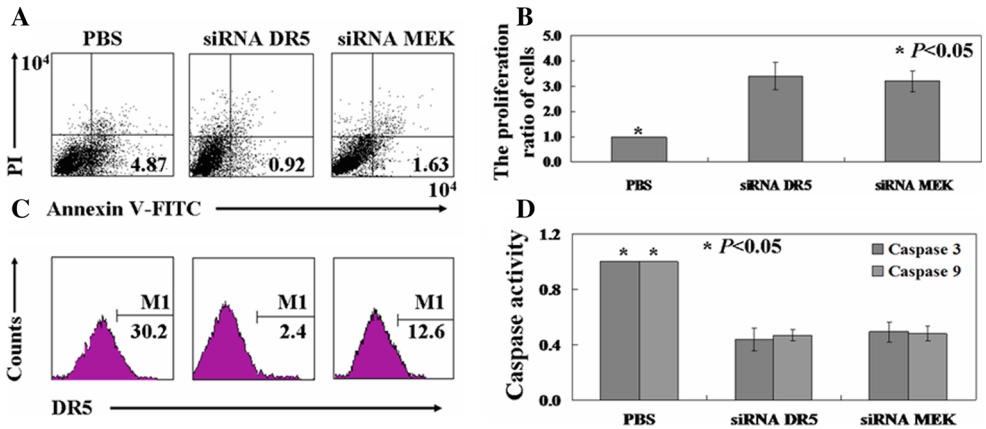

Fig. 6 The role of CLDN7 and TRAIL in CTCs. **a** CTCs in serum of each group were isolated using the CellSearch system. **b** Kaplan–Meier plot estimating overall survival for 3 risk groups (<1 CTCs, 1–5 CTCs, >5 CTCs). **c** Serum TRAIL levels from xenograft mouse models were measured using ELISA. **d** Negative correlation between serum levels of TRAIL and CTCs in xenograft mouse models, when the TRAIL-treated H460-GFP-CLDN7 group was excluded. **e** No correlation between serum levels of TRAIL and CTCs in xenograft mouse models in any treatment group

Fig. 7 CLDN7 moderates the cytotoxicity of TRAIL in H460 cells after siRNA *MEK* or siRNA *TNFRSF10B* treatment in vitro. **a** The proportion of apoptotic cells (early apoptosis) was determined by double-staining with annexin V/FITC and PI. **b** The *growth curve* of cell lines was measured using the MTT assay. **c** The cell surface expressions of TNFRSF10A and TNFRSF10B in H460 cells were detected by flow cytometry. **d** The activity of caspase 3 and 9 was detected in each group

(NSCLCs) had a low CLDN7 expression compared with normal lung tissues. Lu et al. [12] found that CLDN7 was normally expressed in bronchial epithelial cells of human lungs but was either downregulated or disrupted in its distribution pattern in lung cancer. In this work, we also confirmed a low level of CLDN7 in lung cancer H460 cells.

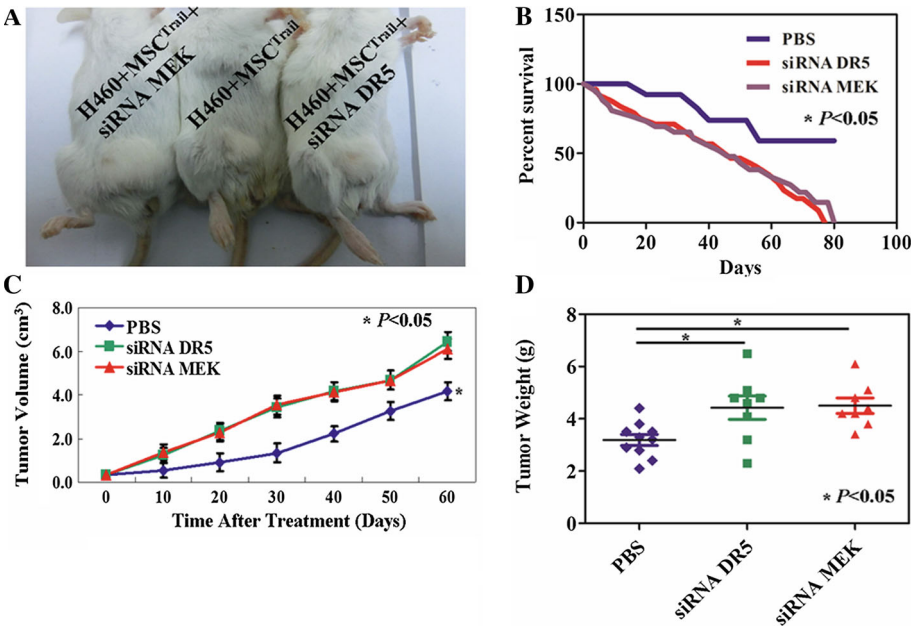

Fig. 8 CLDN7 moderates the cytotoxicity of TRAIL in H460 cells after siRNA *MEK* or siRNA *TNFRSF10B* treatment in vivo. **a** Macroscopic appearance of subcutaneous tumors in each group described in "Materials and methods" section. **b** Kaplan–Meier survival curves of the groups described in "Materials and methods" section. **c**, **d** Tumor volume and tumor weights of each group described in "Materials and methods" section

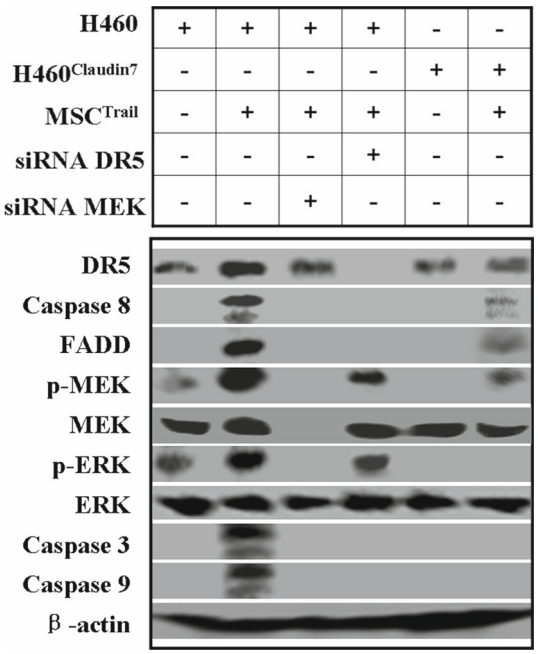

Fig. 9 Western blot analysis of the MEK/ERK signaling pathway and the TRAIL signaling pathway. MEK1/2 and ERK1/2 or their phosphorylation forms, TNFRSF10B, FADD, and caspase 3, 8, and 9 in cell lysates were determined

In addition, to investigate how CLDN7 affects the viability of lung cancer cells, we transfected *CLDN7* tagged with GFP into H460 cells to induce overexpression of CLDN7. Previous research suggests that CLDN7 overexpression induces a loss of polarization, enhances proliferation, and promotes the tumorigenicity of colorectal cancer cells [25]. However, in our study, we found that CLDN7 was associated with a slightly repressive effect on H460 cells. In our view, the inhibitory effect was caused by plasmid transfection, and not by the *CLDN7* gene itself [26].

TRAIL is a member of the TNF super family that has emerged since its discovery in 1995 as a prominent biologically-targeted anti-tumor protein [27]. TRAIL activity as an anti-tumor protein is mediated through its interaction with TRAIL receptors. TRAIL can bind to five receptors, TNFRSF10A/DR4 [28, 29], and TNFRSF10B/TNFRSF10B [30, 31], whereas the other three are decoy receptors. Ouyang et al. [32] found that TRAIL could not increase the total mRNA or protein expression of death receptors but could induce a redistribution into the raft domains on the plasma membrane of TRAIL-sensitive H460 cells. Similar to their results, we found that the levels of *TNFRSF10A* or *TNFRSF10B* mRNA and TNFRSF10A or TNFRSF10B protein did not change significantly after TRAIL treatment. However, although the overall levels of TNFRSF10B did not change, it was redistributed and accumulated in H460 membranes. Interesting, TRAIL was associated with increased TNFRSF10B expression in vivo. The inconsistency may be caused by the microenvironment of tumor cells. Unfortunately, we cannot answer this question with existing data and will address it in our future research.

In this work, we used MSCs as specialized delivery vehicles of TRAIL for treating H460 cells in vitro and in vivo. Consistent with a previous study [33], we also found that, when injected subcutaneously into mice, TRAIL-transduced MSCs were able to localize into tumors and mediate tumor cell apoptosis. Many previous studies have shown the anti-tumor activities of TRAIL in various cancer cells [34–36]. In this work, we confirmed TRAIL-induced apoptosis in H460 cells.

The main purpose of our study was to determine the role of CLDN7 in the cytotoxicity of TRAIL. Adjuvant agents that lower resistance of cancer cells to TRAIL alter the expression of apoptosis inhibitors [37]. Sulforaphane could up-regulate TNFRSF10B expression and enhance TRAIL-induced apoptosis in human osteosarcoma cells [38]. Bisphosphonate enhances TRAIL sensitivity to human osteosarcoma cells via TNFRSF10B up-regulation [39]. The current study showed for the first time that reduction of TRAIL-induced tumoricidal activity in H460 cells was through CLDN7. A further reason is that TNFRSF10B expression was downregulated by CLDN7 in H460 cells. However, co-immunoprecipitation analyses did not indicate a direct interaction between CLDN7 and TRAIL.

Lu et al. [12] found that CLDN7 inhibits human lung cancer cell migration and invasion through the ERK/MAPK signaling pathway. Yan et al. [40] found that bufalin-induced downregulation of Cbl proto-oncogene B (CBLB) contributed to the upregulation of TNFRSF10A and TNFRSF10B, which might be partially mediated by the activation of ERK, JNK and p38 MAPK. Qu et al. [41] found that interferon-α sensitizes human gastric cancer cells to TRAIL-induced apoptosis via activation of the c-Cbl-dependent MAPK/ERK pathway. Our results provide an integrated insight into the mechanism of CLDN7-regulated TRAIL cytotoxicity in H460 cells, in particular, the role of CLDN7-mediated sensitivity of TRAIL via MEK/ERK signaling pathway.

There is another possible mechanism between CLDN7 and TRAIL. A previous study showed that CLDN7 expression was significantly decreased in lichen sclerosus and vulvar squamous-cell carcinoma samples compared with the control group (vulvar tissue without lichen sclerosus or squamous-cell carcinoma), while that of p53 was significantly increased [42]. Additionally, Kulawiec et al. [43] identified tight junction proteins claudin 1 and CLDN7 in the p53 network. Many previous studies have shown that TRAIL-induced apoptosis is associated with p53 [44, 45]. The details of this mechanism will be the focus of our future study.

Another main finding of the present work is the changes in some cytokines in H460 cells after TRAIL treatment. Previous studies have shown that IL8 and IL6 secretion is dependent on activation of the MEK/ERK signaling pathway [46–48]. In this work, we found that CLDN7 could inhibit IL8 and IL6 secretion by suppressing the MEK/ERK signaling pathway. We also found that two tissue metalloproteinases, MMP2 and MMP9, were increased after TRAIL treatment. Increased levels of MMP2 and MMP9 have been associated with the metastasis of many cancers, including colorectal [49], papillary thyroid [50], esophageal [51], and ovarian [52] cancers. A recent study showed that a mitogen-activated protein kinase kinase (MAP2K)/extracellular signal-regulated kinase (ERK) MEK 1/2 inhibitor could inhibit the mRNA expression and protein activities of MMP1, MMP2, and MMP9 through the Ras/MEK/ERK signaling pathway [53]. Consistent with previous studies, we found that CLDN7 could inhibit MMP2 and MMP9 expression by suppressing the MEK/ERK signaling pathway.

In this work, other evidence also confirmed the antitumor activities of TRAIL in H460 cells. CTCs collected from peripheral blood were recently shown to predict disease outcome and therapy response [54–56], and CTC levels have been inversely associated with progression-free and overall survival [57, 58]. The present study notes that mice without or with lower CTCs had a longer survival time than the ones with higher CTCs. Fewer CTCs were isolated from blood samples collected from mice after TRAIL treatment. These data showed the efficacy of TRAIL in mice with H460 xenografts models.

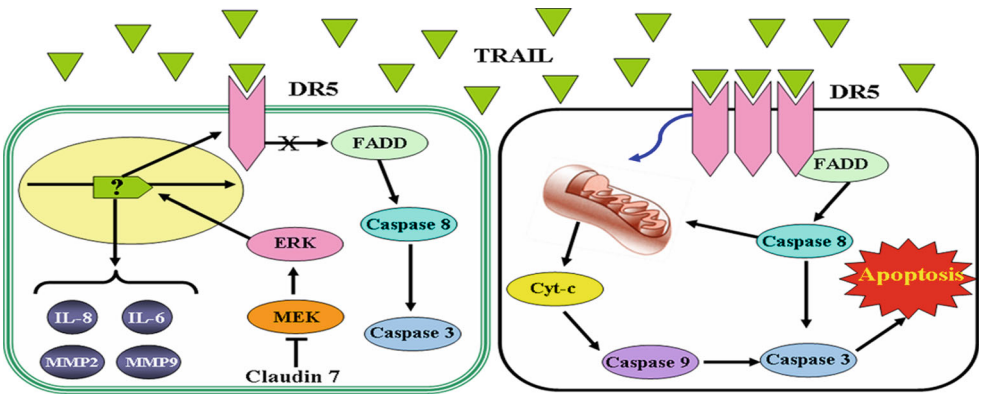

Fig. 10 Schematic model of the mechanism proposed for the decreased sensitivity of H460 cells to TRAIL-induced apoptosis when CLDN7 is overexpressed. CLDN7 inhibits phosphorylated MEK (p-MEK). p-MEK promotes p-ERK and TNFRSF10B expression. Inhibition of MEK/ERK signaling by CLDN7 results in suppressing the cytotoxicity of TRAIL. However, the target transcription factors of ERK remain unclear

Conclusions

In summary, the principal findings of our study are that: (1) TRAIL-mediated apoptosis is regulated by the expression of CLDN7 in vivo and in vitro, (2) CLDN7 inhibits TRAIL-induced apoptosis in H460 cells by suppressing the MEK/ERK signaling pathway, and (3) some cytokines (MMP2 and MMP9) also changed with expression of CLDN7 (Fig. 10). However, although CLDN7 could inhibit the mobility of H460 cells, it is not clear how GFP-tagged CLDN7 in H460 cells attracted TRAIL-transfected MSCs. Furthermore, the DNA-binding proteins involved in the regulation of the transcription of the *TNFRSF10B* gene remain unknown.

Acknowledgments We thank Dr Jin-Jin Wang for providing mesenchymal stem cells.

Conflict of interest The authors declare no conflict of interest.

References

1. Soler AP, Miller RD, Laughlin KV, Carp NZ, Klurfeld DM, Mullin JM (1999) Increased tight junctional permeability is associated with the development of colon cancer. Carcinogenesis 20:1425–1431
2. Tsukita S, Furuse M, Itoh M (2001) Multifunctional strands in tight junctions. Nat Rev Mol Cell Biol 2:285–293
3. Schneeberger EE, Lynch RD (2004) The tight junction: a multifunctional complex. Am J Physiol Cell Physiol 286:C1213–C1228
4. Peacock RE, Keen TJ, Inglehearn CF (1997) Analysis of a human gene homologous to rat ventral prostate.1 protein. Genomics 46:443–449
5. Paschoud S, Bongiovanni M, Pache JC, Citi S (2007) Claudin-1 and claudin-5 expression patterns differentiate lung squamous cell carcinomas from adenocarcinomas. Mod Pathol 20:947–954
6. Moldvay J, Jäckel M, Páska C, Soltész I, Schaff Z, Kiss A (2007) Distinct claudin expression profile in histologic subtypes of lung cancer. Lung Cancer 57:159–167
7. Blackman B, Russell T, Nordeen SK, Medina D, Neville MC (2005) Claudin 7 expression and localization in the normal murine mammary gland and murine mammary tumors. Breast Cancer Res 7:R248–R255
8. Ladwein M, Pape UF, Schmidt DS, Schnölzer M, Fiedler S, Langbein L, Franke WW, Moldenhauer G, Zöller M (2005) The cell–cell adhesion molecule EpCAM interacts directly with the tight junction protein claudin-7. Exp Cell Res 309:345–357
9. Kominsky SL, Argani P, Korz D, Evron E, Raman V, Garrett E, Rein A, Sauter G, Kallioniemi OP, Sukumar S (2003) Loss of the tight junction protein claudin-7 correlates with histological grade in both ductal carcinoma in situ and invasive ductal carcinoma of the breast. Oncogene 22:2021–2033
10. Oshima T, Kunisaki C, Yoshihara K, Yamada R, Yamamoto N, Sato T, Makino H, Yamagishi S, Nagano Y, Fujii S, Shiozawa M, Akaike M, Wada N, Rino Y, Masuda M, Tanaka K, Imada T (2008) Reduced expression of the claudin-7 gene correlates with venous invasion and liver metastasis in colorectal cancer. Oncol Rep 19:953–959
11. Usami Y, Chiba H, Nakayama F, Ueda J, Matsuda Y, Sawada N, Komori T, Ito A, Yokozaki H (2006) Reduced expression of claudin-7 correlates with invasion and metastasis in squamous cell carcinoma of the esophagus. Hum Pathol 37:569–577
12. Lu Z, Ding L, Hong H, Hoggard J, Lu Q, Chen YH (2011) Claudin-7 inhibits human lung cancer cell migration and invasion through ERK/MAPK signaling pathway. Exp Cell Res 317:1935–1946
13. Yamamoto T, Oshima T, Yoshihara K, Yamanaka S, Nishii T, Arai H, Inui K, Kaneko T, Nozawa A, Woo T, Rino Y, Masuda M, Imada T (2010) Reduced expression of claudin-7 is associated with poor outcome in non-small cell lung cancer. Oncol Lett 1:501–505
14. Wiley SR, Schooley K, Smolak PJ, Din WS, Huang CP, Nicholl JK, Sutherland GR, Smith TD, Rauch C, Smith CA et al (1995) Identification and characterization of a new member of the TNF family that induces apoptosis. Immunity 3:673–682
15. Jin Z, McDonald ER 3rd, Dicker DT, El-Deiry WS (2004) Deficient tumor necrosis factor-related apoptosis-inducing ligand (TRAIL) death receptor transport to the cell surface in human colon cancer cells selected for resistance to TRAIL-induced apoptosis. J Biol Chem 279:35829–35839
16. Zhang L, Fang B (2005) Mechanisms of resistance to TRAIL-induced apoptosis in cancer. Cancer Gene Ther 12:228–237
17. Platzbecker U, Kurre P, Guardiola P, Ward JL, Radich JP, Kiem HP, Deeg HJ (2004) Fanconi anemia type C-deficient hematopoietic cells are resistant to TRAIL (TNF-related apoptosis-inducing ligand)-induced cleavage of pro-caspase-8. Exp Hematol 32:815–821
18. Sun SY, Yue P, Zhou JY, Wang Y, Choi Kim HR, Lotan R, Wu GS (2001) Overexpression of BCL2 blocks TNF-related apoptosis-inducing ligand (TRAIL)-induced apoptosis in human lung cancer cells. Biochem Biophys Res Commun 280:788–797
19. Mahalingam D, Szegezdi E, Keane M, de Jong S, Samali A (2009) TRAIL receptor signalling and modulation: Are we on the right TRAIL? Cancer Treat Rev 35:280–288
20. Hori T, Kondo T, Kanamori M, Tabuchi Y, Ogawa R, Zhao QL, Ahmed K, Yasuda T, Seki S, Suzuki K, Kimura T (2010) Ionizing radiation enhances tumor necrosis factor-related apoptosis-inducing ligand (TRAIL)-induced apoptosis through up-regulations of death receptor 4 (DR4) and death receptor 5 (DR5) in human osteosarcoma cells. J Orthop Res 28:739–745
21. Studeny M, Marini FC, Champlin RE, Zompetta C, Fidler IJ, Andreeff M (2002) Bone marrow-derived mesenchymal stem cells as vehicles for interferon-beta delivery into tumors. Cancer Res 62:3603–3608
22. Loebinger MR, Eddaoudi A, Davies D, Janes SM (2009) Mesenchymal stem cell delivery of TRAIL can eliminate metastatic cancer. Cancer Res 69:4134–4142
23. Alessandri G, Filippeschi S, Sinibaldi P, Mornet F, Passera P, Spreafico F, Cappa PM, Gullino PM (1987) Influence of gangliosides on primary and metastatic neoplastic growth in human and murine cells. Cancer Res 47:4243–4247
24. Allard WJ, Matera J, Miller MC, Repollet M, Connelly MC, Rao C, Tibbe AG, Uhr JW, Terstappen LW (2004) Tumor cells circulate in the peripheral blood of all major carcinomas but not in healthy subjects or patients with nonmalignant diseases. Clin Cancer Res 10:6897–6904
25. Darido C, Buchert M, Pannequin J, Bastide P, Zalzali H, Mantamadiotis T, Bourgaux JF, Garambois V, Jay P, Blache P, Joubert D, Hollande F (2008) Defective claudin-7 regulation by Tcf-4 and Sox-9 disrupts the polarity and increases the tumorigenicity of colorectal cancer cells. Cancer Res 68:4258–4268
26. Ou M, Wang XL, Xu R, Chang CW, Bull DA, Kim SW (2008) Novel biodegradable poly(disulfide amine)s for gene delivery

with high efficiency and low cytotoxicity. Bioconjug Chem 19:626–633
27. Walczak H, Miller RE, Ariail K, Gliniak B, Griffith TS, Kubin M, Chin W, Jones J, Woodward A, Le T, Smith C, Smolak P, Goodwin RG, Rauch CT, Schuh JC, Lynch DH (1999) Tumoricidal activity of tumor necrosis factor-related apoptosis-inducing ligand in vivo. Nat Med 5:157–163
28. MacFarlane M, Ahmad M, Srinivasula SM, Fernandes-Alnemri T, Cohen GM, Alnemri ES (1997) Identification and molecular cloning of two novel receptors for the cytotoxic ligand TRAIL. J Biol Chem 272:25417–25420
29. Sheridan JP, Marsters SA, Pitti RM, Gurney A, Skubatch M, Baldwin D, Ramakrishnan L, Gray CL, Baker K, Wood WI, Goddard AD, Godowski P, Ashkenazi A (1997) Control of TRAIL-induced apoptosis by a family of signaling and decoy receptors. Science 277:818–821
30. Pan G, Ni J, Wei YF, Yu G, Gentz R, Dixit VM (1997) An antagonist decoy receptor and a death domain-containing receptor for TRAIL. Science 277:815–818
31. Wu GS, Burns TF, Zhan Y, Alnemri ES, El-Deiry WS (1999) Molecular cloning and functional analysis of the mouse homologue of the KILLER/DR5 tumor necrosis factor-related apoptosis-inducing ligand (TRAIL) death receptor. Cancer Res 59: 2770–2775
32. Ouyang W, Yang C, Liu Y, Xiong J, Zhang J, Zhong Y, Zhang G, Zhou F, Zhou Y, Xie C (2011) Redistribution of DR4 and DR5 in lipid rafts accounts for the sensitivity to TRAIL in NSCLC cells. Int J Oncol 39:1577–1586
33. Grisendi G, Bussolari R, Cafarelli L, Petak I, Rasini V, Veronesi E, De Santis G, Spano C, Tagliazzucchi M, Barti-Juhasz H, Scarabelli L, Bambi F, Frassoldati A, Rossi G, Casali C, Morandi U, Horwitz EM, Paolucci P, Conte P, Dominici M (2010) Adipose-derived mesenchymal stem cells as stable source of tumor necrosis factor-related apoptosis-inducing ligand delivery for cancer therapy. Cancer Res 70:3718–3729
34. Ashkenazi A, Pai RC, Fong S, Leung S, Lawrence DA, Marsters SA, Blackie C, Chang L, McMurtrey AE, Hebert A, DeForge L, Koumenis IL, Lewis D, Harris L, Bussiere J, Koeppen H, Shahrokh Z, Schwall RH (1999) Safety and antitumor activity of recombinant soluble Apo2 ligand. J Clin Invest 104:155–162
35. French LE, Tschopp J (1999) The TRAIL to selective tumor death. Nat Med 5:146–147
36. Chae SY, Kim TH, Park K, Jin CH, Son S, Lee S, Youn YS, Kim K, Jo DG, Kwon IC, Chen X, Lee KC (2010) Improved antitumor activity and tumor targeting of NH(2)-terminal-specific PEGylated tumor necrosis factor-related apoptosis-inducing ligand. Mol Cancer Ther 9:1719–1729
37. Mirandola P, Sponzilli I, Gobbi G, Marmiroli S, Rinaldi L, Binazzi R, Piccari GG, Ramazzotti G, Gaboardi GC, Cocco L, Vitale M (2006) Anticancer agents sensitize osteosarcoma cells to TNF-related apoptosis-inducing ligand downmodulating IAP family proteins. Int J Oncol 28:127–133
38. Matsui TA, Sowa Y, Yoshida T, Murata H, Horinaka M, Wakada M, Nakanishi R, Sakabe T, Kubo T, Sakai T (2006) Sulforaphane enhances TRAIL-induced apoptosis through the induction of DR5 expression in human osteosarcoma cells. Carcinogenesis 27:1768–1777
39. Moon MH, Jeong JK, Seo JS, Seol JW, Lee YJ, Xue M, Jackson CJ, Park SY (2011) Bisphosphonate enhances TRAIL sensitivity to human osteosarcoma cells via death receptor 5 upregulation. Exp Mol Med 43:138–145
40. Yan S, Qu X, Xu C, Zhu Z, Zhang L, Xu L, Song N, Teng Y, Liu Y (2012) Down-regulation of Cbl-b by bufalin results in up-regulation of DR4/DR5 and sensitization of TRAIL-induced apoptosis in breast cancer cells. J Cancer Res Clin Oncol 138: 1279–1289
41. Qu J, Zhao M, Teng Y, Zhang Y, Hou K, Jiang Y, Yang X, Shang H, Qu X, Liu Y (2011) Interferon-α sensitizes human gastric cancer cells to TRAIL-induced apoptosis via activation of the c-CBL-dependent MAPK/ERK pathway. Cancer Biol Ther 12: 494–502
42. Sadalla JC, Lourenço SV, Sotto MN, Baracat EC, Carvalho JP (2011) Claudin and p53 expression in vulvar lichen sclerosus and squamous-cell carcinoma. J Clin Pathol 64:853–857
43. Kulawiec M, Safina A, Desouki MM, Still I, Matsui S, Bakin A, Singh KK (2008) Tumorigenic transformation of human breast epithelial cells induced by mitochondrial DNA depletion. Cancer Biol Ther 7:1732–1743
44. Yu R, Deedigan L, Albarenque SM, Mohr A, Zwacka RM (2013) Delivery of sTRAIL variants by MSCs in combination with cytotoxic drug treatment leads to p53-independent enhanced antitumor effects. Cell Death Dis 4:e503
45. Park EJ, Choi KS, Yoo YH, Kwon TK (2013) Nutlin-3, a small-molecule MDM2 inhibitor, sensitizes Caki cells to TRAIL-induced apoptosis through p53-mediated PUMA upregulation and ROS-mediated DR5 upregulation. Anticancer Drugs 24:260–269
46. Tang H, Sun Y, Shi Z, Huang H, Fang Z, Chen J, Xiu Q, Li B (2013) YKL-40 induces IL-8 expression from bronchial epithelium via MAPK (JNK and ERK) and NF-κB pathways, causing bronchial smooth muscle proliferation and migration. J Immunol 190:438–446
47. Maza PK, Oliveira P, Toledo MS, Paula DM, Takahashi HK, Straus AH, Suzuki E (2012) Paracoccidioides brasiliensis induces secretion of IL-6 and IL-8 by lung epithelial cells. Modulation of host cytokine levels by fungal proteases. Microbes Infect 14:1077–1085
48. Yin J, Yu C, Yang Z, He JL, Chen WJ, Liu HZ, Li WM, Liu HT, Wang YX (2011) Tetramethylpyrazine inhibits migration of SKOV3 human ovarian carcinoma cells and decreases the expression of interleukin-8 via the ERK1/2, p38 and AP-1 signaling pathways. Oncol Rep 26:671–679
49. Holten-Andersen MN, Hansen U, Brünner N, Nielsen HJ, Illemann M, Nielsen BS (2005) Localization of tissue inhibitor of metalloproteinases 1 (TIMP-1) in human colorectal adenoma and adenocarcinoma. Int J Cancer 113:198–206
50. Bommarito A, Richiusa P, Carissimi E, Pizzolanti G, Rodolico V, Zito G, Criscimanna A, Di Blasi F, Pitrone M, Zerilli M, Amato MC, Spinelli G, Carina V, Modica G, Latteri MA, Galluzzo A, Giordano C (2011) BRAFV600E mutation, TIMP-1 upregulation, and NF-κB activation: closing the loop on the papillary thyroid cancer trilogy. Endocr Relat Cancer 18:669–685
51. Groblewska M, Mroczko B, Kozlowski M, Niklinski J, Laudanski J, Szmitkowski M (2012) Serum matrix metalloproteinase 2 and tissue inhibitor of matrix metalloproteinases 2 in esophageal cancer patients. Folia Histochem Cytobiol 50:590–598
52. Hałoń A, Nowak-Markwitz E, Donizy P, Matkowski R, Maciejczyk A, Gansukh T, Györffy B, Spaczyński M, Zabel M, Lage H, Surowiak P (2012) Enhanced immunoreactivity of TIMP-2 in the stromal compartment of tumor as a marker of favorable prognosis in ovarian cancer patients. J Histochem Cytochem 60: 491–501
53. Tsubaki M, Satou T, Itoh T, Imano M, Ogaki M, Yanae M, Nishida S (2012) Reduction of metastasis, cell invasion, and adhesion in mouse osteosarcoma by YM529/ONO-5920-induced blockade of the Ras/MEK/ERK and Ras/PI3K/Akt pathway. Toxicol Appl Pharmacol 259:402–410
54. Gasent Blesa JM, Alberola Candel V, Esteban González E, Vidal Martínez J, Gisbert Criado R, Provencio Pulla M, Laforga Canales J, Pachmann K (2008) Circulating tumor cells in breast cancer: methodology and clinical repercussions. Clin Transl Oncol 10:399–406
55. Goodman OB Jr, Fink LM, Symanowski JT, Wong B, Grobaski B, Pomerantz D, Ma Y, Ward DC, Vogelzang NJ (2009)

Circulating tumor cells in patients with castration-resistant prostate cancer baseline values and correlation with prognostic factors. Cancer Epidemiol Biomarkers Prev 18:1904–1913

56. Ignatiadis M, Xenidis N, Perraki M, Apostolaki S, Politaki E, Kafousi M, Stathopoulos EN, Stathopoulou A, Lianidou E, Chlouverakis G, Sotiriou C, Georgoulias V, Mavroudis D (2007) Different prognostic value of cytokeratin-19 mRNA positive circulating tumor cells according to estrogen receptor and HER2 status in early-stage breast cancer. J Clin Oncol 25:5194–5202
57. Cohen SJ, Punt CJ, Iannotti N, Saidman BH, Sabbath KD, Gabrail NY, Picus J, Morse M, Mitchell E, Miller MC, Doyle GV, Tissing H, Terstappen LW, Meropol NJ (2008) Relationship of circulating tumor cells to tumor response, progression-free survival, and overall survival in patients with metastatic colorectal cancer. J Clin Oncol 26:3213–3221
58. de Bono JS, Scher HI, Montgomery RB, Parker C, Miller MC, Tissing H, Doyle GV, Terstappen LW, Pienta KJ, Raghavan D (2008) Circulating tumor cells predict survival benefit from treatment in metastatic castration-resistant prostate cancer. Clin Cancer Res 14:6302–6309